Electronic Supplementary Material (ESI) for ChemComm.
This journal is © The Royal Society of Chemistry 2024

SUPPORTING INFORMATION

D_{4h} H©$K_4H_4^-$: A Planar Tetracoordinate Hydrogen Global Minimum

Li-Xia Bai, Yan-Xia Jin, and Jin-Chang Guo*

Key Laboratory of Materials for Energy Conversion and Storage of Shanxi Province,

Institute of Molecular Science, Shanxi University, Taiyuan 030006, China

*E-mail: guojc@sxu.edu.cn

Supporting Information

Table S1. The lowest vibrational frequency (in cm^{-1}) at eight theoretical levels for the global-minimum structure **1** (D_{4h}, $^1A_{1g}$) of H©$K_4H_4^-$ cluster.

Table S2. Energy components of IQA for **1** at the PBE0/TZ2P level; Vint IQA, Vint C, and Vint XC are the interatomic IQA interaction energy, the coulombic and exchange-correlation energy components, respectively, in kcal mol^{-1}.

Table S3. Composition analysis of canonical molecular orbitals (CMOs) for the GM (**1**) structure of H©$K_4H_4^-$ at the PBE0/def2-TZVPP level.

Figure S1. Optimized structures of D_{4h} H©$M_4H_4^-$ (M = Li, Na, Rb, Cs) at the PBE0-D3(BJ)/def2-TZVPP level. The lowest frequencies (in cm^{-1}) and the numbers of imaginary frequencies (NIMG) are shown.

Figure S2. Optimized structures of H©$K_4H_4^-$ at the CCSD/def2-TZVPP (a) and CCSD(T)/def2-TZVPP (b) levels. The bond distances (in Å) and the lowest frequencies (in cm^{-1}) are shown.

Figure S3. Optimized structures for the top 20 low-lying isomers of $K_4H_5^-$ at the PBE0-

D3(BJ)/def2-TZVPP level. Relative energies are listed in kcal/mol at the single-point CCSD(T)/def2-TZVPP//PBE0-D3(BJ)/def2-TZVPP levels, with zero-point energy (ZPE) corrections at PBE0-D3(BJ)/def2-TZVPP. The T1 diagnostic values are listed.

Figure S4. Optimized structure of the most stable triplet structure of $K_4H_5^-$ with dissociation at PBE0-D3(BJ)/def2-TZVPP level. The most stable triplet structure without dissociation is also depictured. Relative energies are listed in kcal mol^{-1} at the single-point CCSD(T)/def2-TZVPP//PBE0-D3(BJ)/def2-TZVPP levels, with zero-point energy (ZPE) corrections at PBE0-D3(BJ)/def2-TZVPP. The T1 diagnostic values are listed.

Figure S5. Optimized structure of K_4H_4 at the PBE0-D3(BJ)/def2-TZVPP level. The bond distances (in Å), Wiberg bond orders (blue color), and NPA charges (in |e|, red color) are shown.

Figure S6. (a) The ELF contour map of **1**. (b) The plot of the Laplacian of electron density, bond paths and critical points. The red dashed lines denote the areas of charge concentration ($\nabla^2\rho(r) < 0$) and the blue area is vice versa. The brown sticks between the atoms represent bond paths. The brown and yellow dots are bond and ring critical points, respectively.

Figure S7. Color-filled maps of $NICS(0)_{zz}$ for the **1** cluster. Negative values indicate aromaticity. 0 in parentheses represent the height above the molecular plane (in Å). The blue ring indicates the interface with the $NICS_{zz}$ values of 0.

Figure S8. The canonical molecular orbital energy diagram of **1**.

Cartesian coordinates of the top 20 low-lying isomers of $K_4H_5^-$ at the PBE0-D3(BJ)/def2-TZVPP level.

Table S1. The lowest vibrational frequency (in cm^{-1}) at eight theoretical levels for the global-minimum structure **1** (D_{4h}, $^1A_{1g}$) of $H©K_4H_4^-$ cluster.

Theoretical level	Lowest vibrational frequency (cm^{-1})
PBE0-D3(BJ)/def2-TZVPP	29.3
BP86-D3(BJ)/def2-TZVPP	25.6
B3LYP-D3(BJ)/def2-TZVPP	27.1
B3PW91-D3(BJ)/def2-TZVPP	26.4
TPSS-D3(BJ)/def2-TZVPP	26.4
MP2/def2-TZVPP	27.3
M06-2X/def2-TZVPP	42.8
TPSSh/def2-TZVPP	27.5

Table S2. Energy components of IQA for **1** at the PBE0/TZ2P level; Vint IQA, Vint C, and Vint XC are the interatomic IQA interaction energy, the coulombic and exchange-correlation energy components, respectively, in kcal mol^{-1}.

	$HK_4H_4^-$
Vint IQA (H–K)	–91.77
Vint C (H–K)	–78.98 (86.06%)
Vint XC (H–K)	–12.79 (13.94%)
Vint IQA (K–K)	55.57
Vint C (K–K)	56.51 (98.36%)
Vint XC (K–K)	–0.94 (1.64%)
Vint IQA (H^a–K)	–98.17
Vint C (H^a–K)	–80.15 (81.64%)
Vint XC (H^a–K)	–18.02 (18.36%)

[a]H represents the H atoms at the periphery.

Table S3. Composition analysis of canonical molecular orbitals (CMOs) for the GM (**1**) structure of H©$K_4H_4^-$ at the PBE0/def2-TZVPP level.

CMO	H (%)	H^a_4 (%)	K_4 (%)	
	s	s	s/p/d	total
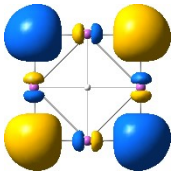 HOMO (b_{2g})	0.00	**88.25**	0.00/9.54/0.00	9.54
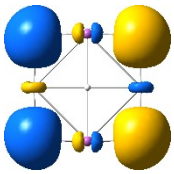 HOMO−1 (e_u)	0.00	**84.38**	7.46/5.30/0.00	12.76
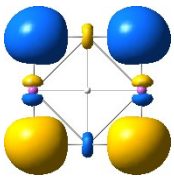 HOMO−1′ (e_u)	0.00	**84.38**	7.46/5.30/0.00	12.76
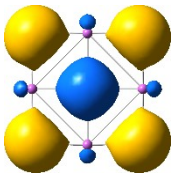 HOMO−2 (a_{1g})	**25.80**	**64.38**	3.38/2.03/3.54	8.95
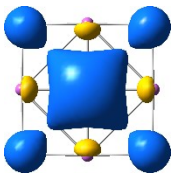 HOMO−3 (a_{1g})	**57.38**	18.98	16.00/3.31/0.00	19.31

[a]H represents the H atoms at the periphery.

Figure S1. Optimized structures of D_{4h} H©$M_4H_4^-$ (M = Li, Na, Rb, Cs) at the PBE0-D3(BJ)/def2-TZVPP level. The lowest frequencies (in cm^{-1}) and the numbers of imaginary frequencies (NIMG) are shown.

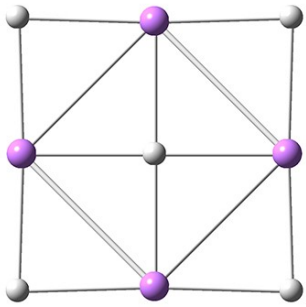

$HLi_4H_4^-$ (D_{4h}, $^1A_{1g}$)
287.0i (NIMG 1)

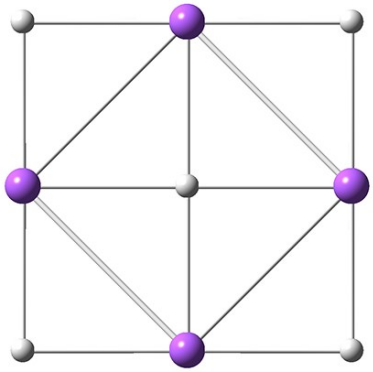

$HNa_4H_4^-$ (D_{4h}, $^1A_{1g}$)
191.2i (NIMG 1)

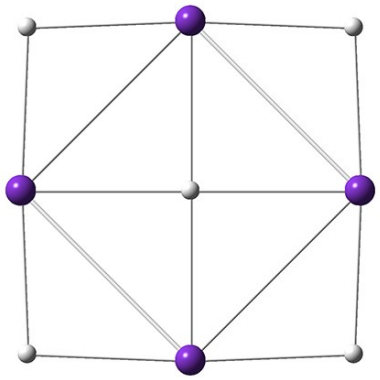

$HRb_4H_4^-$ (D_{4h}, $^1A_{1g}$)
92.3i (NIMG 2)

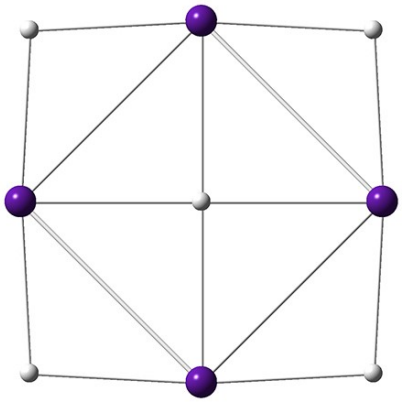

$HCs_4H_4^-$ (D_{4h}, $^1A_{1g}$)
161.9i (NIMG 5)

Figure S2. Optimized structures of $H©K_4H_4^-$ at the CCSD/def2-TZVPP (a) and CCSD(T)/def2-TZVPP (b) levels. The bond distances (in Å) and the lowest frequencies (in cm^{-1}) are shown.

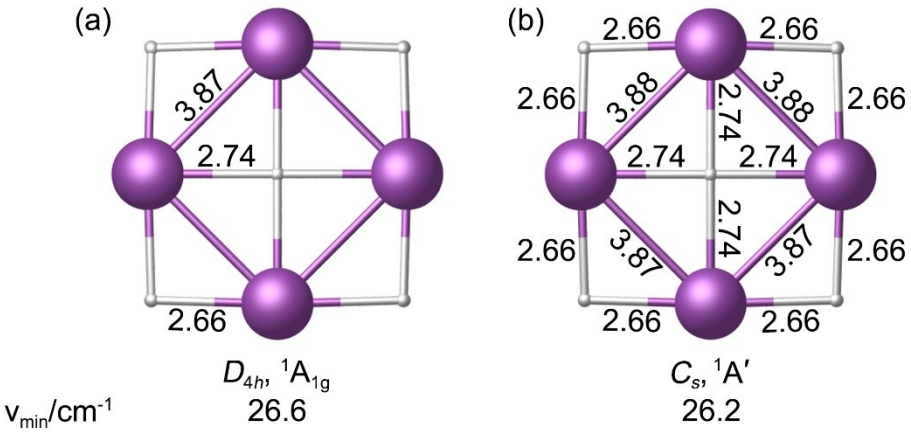

Figure S3. Optimized structures for the top 20 low-lying isomers of $K_4H_5^-$ at the PBE0-D3(BJ)/def2-TZVPP level. Relative energies are listed in kcal/mol at the single-point CCSD(T)/def2-TZVPP//PBE0-D3(BJ)/def2-TZVPP levels, with zero-point energy (ZPE) corrections at PBE0-D3(BJ)/def2-TZVPP. The T1 diagnostic values are listed.

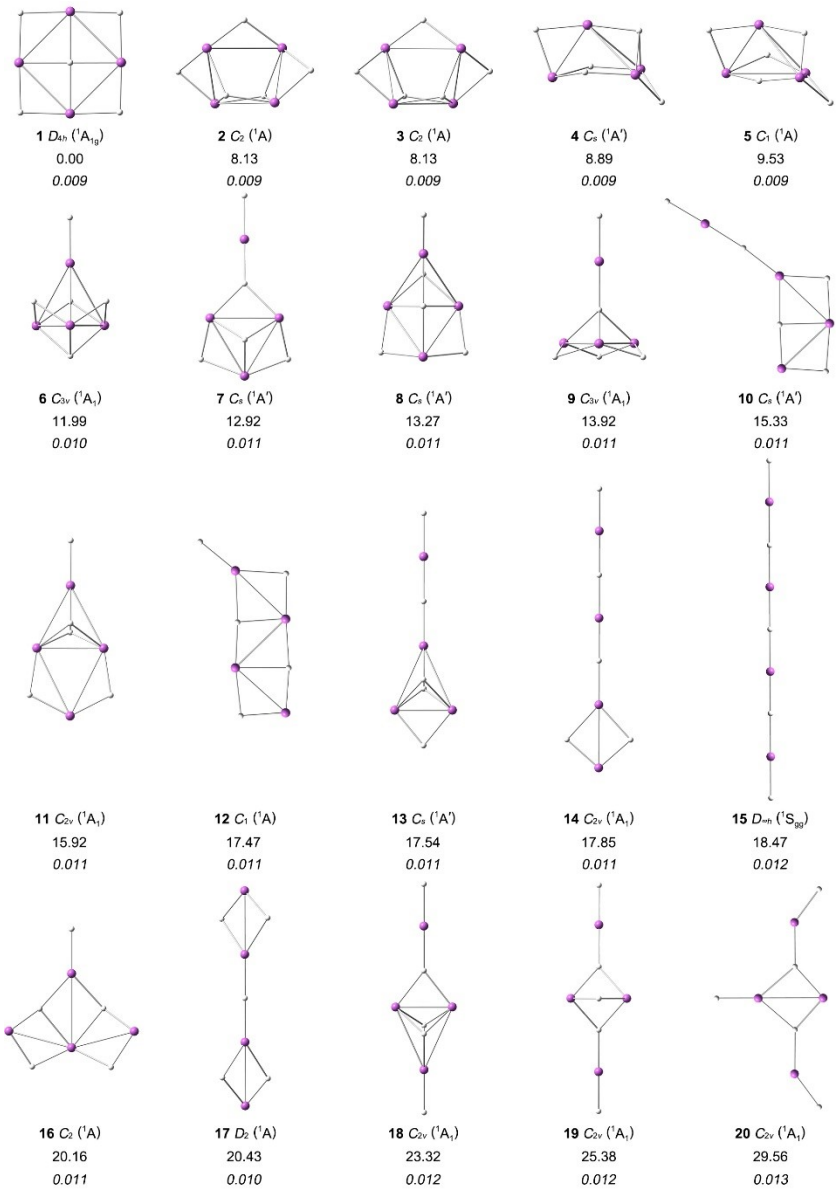

Figure S4. Optimized structure of the most stable triplet structure of $K_4H_5^-$ with dissociation at PBE0-D3(BJ)/def2-TZVPP level. The most stable triplet structure without dissociation is also depictured. Relative energies are listed in kcal mol^{-1} at the single-point CCSD(T)/def2-TZVPP//PBE0-D3(BJ)/def2-TZVPP levels, with zero-point energy (ZPE) corrections at PBE0-D3(BJ)/def2-TZVPP. The T1 diagnostic values are listed.

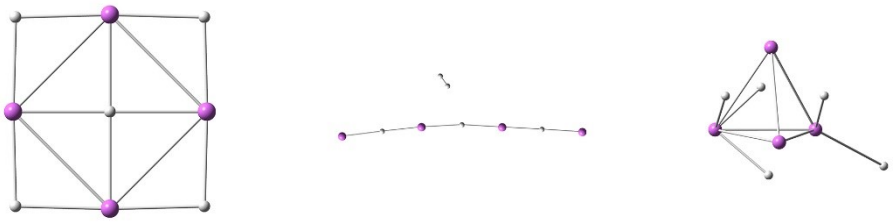

1 D_{4h} ($^1A_{1g}$)
0.00
0.009

C_s ($^3A'$)
9.41
0.009

C_1 (^3A)
62.20
0.019

Figure S5. Optimized structure of K_4H_4 at the PBE0-D3(BJ)/def2-TZVPP level. The bond distances (in Å), Wiberg bond orders (blue color), and NPA charges (in |e|, red color) are shown.

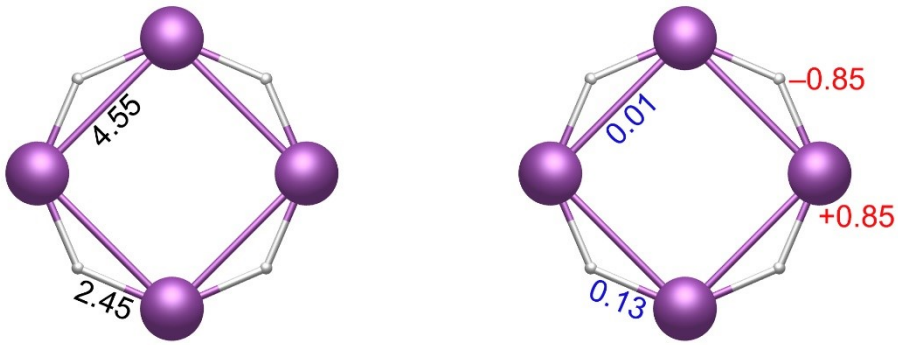

2 K_4H_4 (D_{4h}, $^1A_{1g}$)

Figure S6. (a) The ELF contour map of **1**. (b) The plot of the Laplacian of electron density, bond paths and critical points. The red dashed lines denote the areas of charge concentration ($\nabla^2\rho(r) < 0$) and the blue area is vice versa. The brown sticks between the atoms represent bond paths. The brown and yellow dots are bond and ring critical points, respectively.

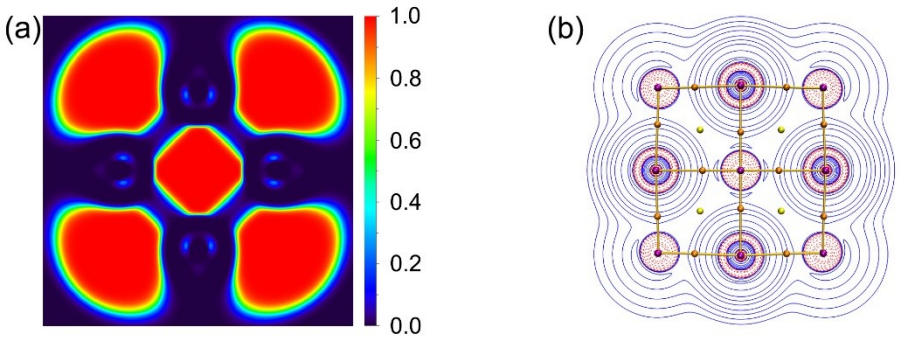

Figure S7. Color-filled maps of $NICS(0)_{zz}$ for the **1** cluster. Negative values indicate aromaticity. 0 in parentheses represent the height above the molecular plane (in Å). The blue ring indicates the interface with the $NICS_{zz}$ values of 0.

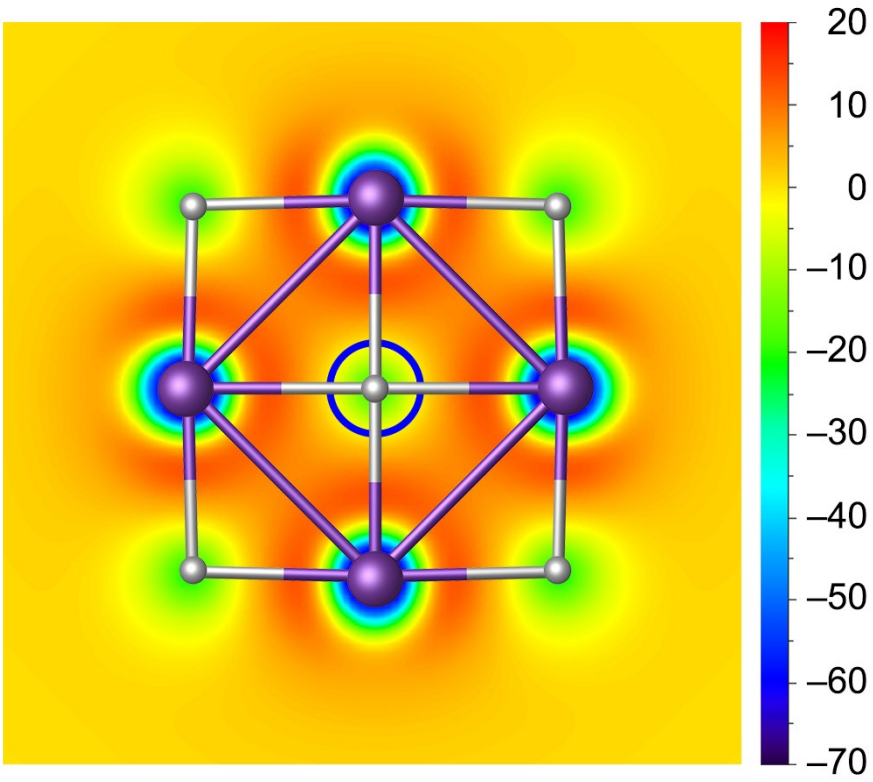

Figure S8. The canonical molecular orbital energy diagram of **1**.

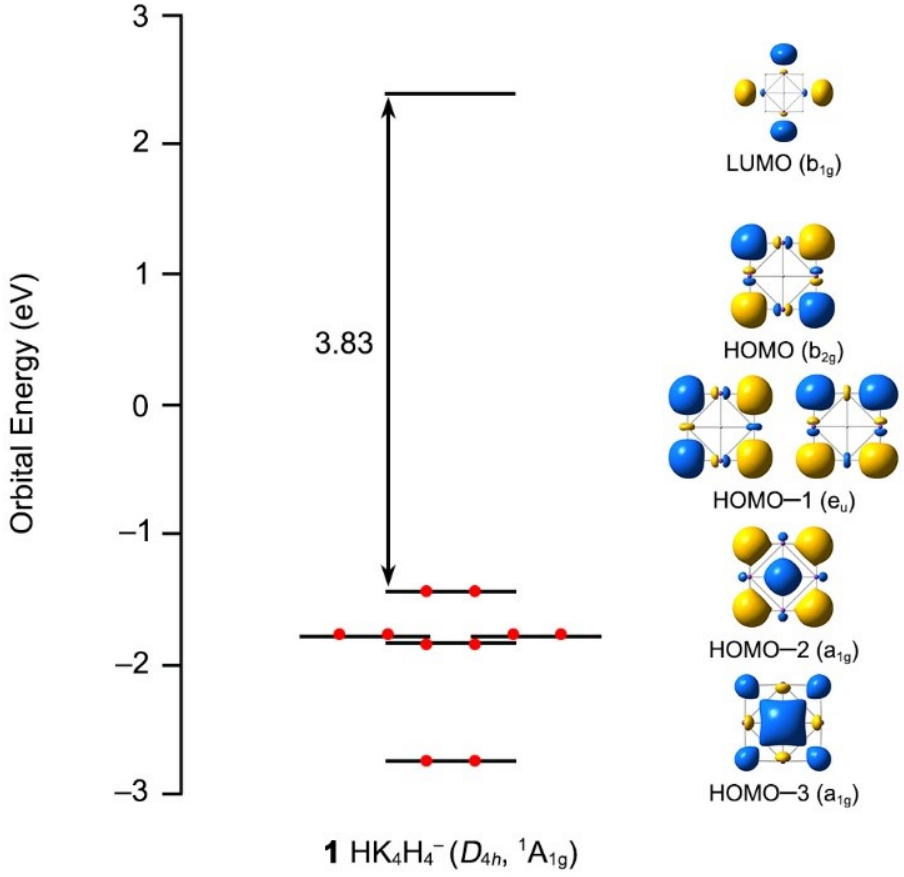

Cartesian coordinates of the top 20 low-lying isomers of $K_4H_5^-$ at the PBE0-D3(BJ)/def2-TZVPP level.

1 H©$K_4H_4^-$ (D_{4h}, $^1A_{1g}$)

K	0.00000000	2.65957600	0.00000000
K	2.65957600	0.00000000	0.00000000
K	0.00000000	-2.65957600	0.00000000
K	-2.65957600	0.00000000	0.00000000
H	-2.59300500	2.59300500	0.00000000
H	2.59300500	2.59300500	0.00000000
H	-2.59300500	-2.59300500	0.00000000
H	2.59300500	-2.59300500	0.00000000
H	0.00000000	0.00000000	0.00000000

2 (C_2, ^1A)

K	-0.91133461	1.87855438	1.41688610
K	0.91133461	-1.87855438	1.41688610
K	0.98725991	1.66691128	-1.44838871
K	-0.98725991	-1.66691128	-1.44838871
H	-0.71965531	-3.55190959	0.22583368
H	0.00000000	0.00000000	2.88318503
H	1.55061510	-0.83588022	-1.06887650
H	-1.55061510	0.83588022	-1.06887650
H	0.71965531	3.55190959	0.22583368

3 (C_2, ^1A)

K	-1.09309033	1.89512365	-1.60586294
K	1.00237929	2.15830455	1.56807826
K	1.09309033	-1.89512365	-1.60586294
K	-1.00237929	-2.15830455	1.56807826
H	-0.87056421	4.18656474	0.28960649
H	0.00000000	0.00000000	3.36403499
H	-1.86715307	-1.01684379	-1.25371501
H	0.87056421	-4.18656474	0.28960649
H	1.86715307	1.01684379	-1.25371501

4 (C_s, $^1A'$)

K	-1.69942049	1.12071329	0.00000000
K	0.23676804	-1.79179953	1.70948474
K	0.23676804	-1.79179953	-1.70948474
K	1.23918677	2.44191741	0.00000000

H	-1.03021362	3.66256140	0.00000000
H	0.53824023	0.73677892	1.85864304
H	-1.83534948	-1.50454086	0.00000000
H	0.53824023	0.73677892	-1.85864304
H	1.53633787	-3.23317977	0.00000000

5 (C_1, ^{1}A)

K	0.79329900	1.00089800	1.42857700
K	-0.68630200	-1.83327400	0.44228100
K	2.61456300	-0.03389500	-1.13368100
K	-2.73367200	0.86380000	-0.69617000
H	4.12206900	1.81320900	-0.51307800
H	1.85598500	-1.51269100	0.91911300
H	-0.00773500	0.40625500	-0.91916500
H	-4.01443500	-0.76704800	-1.89467200
H	-1.72576600	0.10722500	1.62867800

6 (C_{3v}, ^{1}A$_1$)

K	2.08001747	-1.20089865	0.95948315
K	-0.00000000	-0.00000000	-2.66414712
K	-2.08001747	-1.20089865	0.95948315
K	-0.00000000	2.40179729	0.95948315
H	-2.29950786	1.32762148	-0.66466321
H	2.29950786	1.32762148	-0.66466321
H	0.00000000	-0.00000000	-4.99414011
H	0.00000000	-2.65524296	-0.66466321
H	0.00000000	-0.00000000	2.91638552

7 (C_s, ^{1}A′)

K	0.49691549	-3.83576467	0.00000000
K	-0.43578474	-0.46892872	2.06222364
K	-0.43578474	-0.46892872	-2.06222364
K	0.32668195	4.71304872	0.00000000
H	0.32268817	7.04304530	0.00000000
H	0.03078488	1.76141139	0.00000000
H	-2.06838813	-2.04625187	0.00000000
H	1.31319183	-2.80365523	2.72049214
H	1.31319183	-2.80365523	-2.72049214

8 (C_s, ^{1}A′)

K	0.79715011	3.16758863	0.00000000
K	-0.92599479	-0.09558743	-2.12171334
K	-0.92599479	-0.09558743	2.12171334
K	1.03238279	-3.04027339	0.00000000

H	1.85216826	5.24504780	0.00000000
H	1.39274581	0.07806706	0.00000000
H	-0.37635925	-2.96473452	2.66905463
H	-0.37635925	-2.96473452	-2.66905463
H	-2.06551855	1.81968691	0.00000000

9 (C_{3v}, $^1A_1$)

K	0.00000000	2.37581750	-1.28319460
K	-2.05751831	-1.18790875	-1.28319460
K	-0.00000000	0.00000000	3.81170104
K	2.05751831	-1.18790875	-1.28319460
H	0.00000000	0.00000000	0.82913690
H	0.00000000	0.00000000	6.14169681
H	2.77173697	1.60026309	-2.08368711
H	-2.77173697	1.60026309	-2.08368711
H	0.00000000	-3.20052618	-2.08368711

10 (C_s, $^1A'$)

K	0.72141893	-0.96092699	0.00000000
K	5.53262094	0.46500499	0.00000000
K	-3.39372605	2.08536503	0.00000000
K	-3.04702707	-1.53395097	0.00000000
H	7.81560894	1.31768698	0.00000000
H	3.16145294	-0.34562300	0.00000000
H	-1.40244006	0.68420602	0.00000000
H	-5.02258906	0.25353303	0.00000000
H	-1.00448108	-2.96415199	0.00000000

11 (C_{2v}, $^1A_1$)

K	0.72141893	-0.96092699	0.00000000
K	5.53262094	0.46500499	0.00000000
K	-3.39372605	2.08536503	0.00000000
K	-3.04702707	-1.53395097	0.00000000
H	7.81560894	1.31768698	0.00000000
H	3.16145294	-0.34562300	0.00000000
H	-1.40244006	0.68420602	0.00000000
H	-5.02258906	0.25353303	0.00000000
H	-1.00448108	-2.96415199	0.00000000

12 (C_1, ^1A)

K	0.37041100	2.31206200	0.62732000
K	3.61790400	-0.27465700	-0.13373100
K	-1.67687600	-1.35900200	1.06275800
K	-4.59515100	0.30901900	-1.36099700

H	5.00007667	-2.05174946	-0.73409848
H	1.07644800	-0.42932100	1.74753800
H	2.81341200	2.60972500	-0.97592000
H	-2.57319800	1.63366300	0.30857400
H	-4.11747000	-2.41190000	-0.41104400

13 (C_s, ^{1}A′)

K	-6.23666199	-0.21296631	0.00000000
K	3.46465901	-0.17285152	-1.76786883
K	-0.56256387	0.58298171	0.00000000
K	3.46465901	-0.17285152	1.76786883
H	-8.43767435	-0.97745476	0.00000000
H	-3.48504137	0.82219286	0.00000000
H	2.15807613	2.04941672	0.00000000
H	1.44218627	-1.75400913	0.00000000
H	5.85070230	-0.60208034	0.00000000

14 (C_{2v}, ^{1}A$_1$)

K	0.00000000	-0.00000000	6.48792820
K	0.00000000	-0.00000000	-2.08634080
K	0.00000000	-0.00000000	-7.07106280
K	0.00000000	-0.00000000	2.87643920
H	0.00000000	-0.00000000	-9.48799180
H	0.00000000	-0.00000000	-4.55052880
H	0.00000000	-0.00000000	0.35762420
H	0.00000000	-1.82791412	4.87429216
H	-0.00000000	1.82791412	4.87429216

15 ($D_{\infty h}$, $^1\Sigma_{gg}$)

K	0.00000000	0.00000000	-2.46486600
K	0.00000000	0.00000000	2.46486600
K	0.00000000	0.00000000	-7.42813600
K	0.00000000	0.00000000	7.42813600
H	0.00000000	0.00000000	4.90177300
H	0.00000000	0.00000000	0.00000000
H	-0.00000000	0.00000000	-4.90177300
H	0.00000000	0.00000000	-9.83483600
H	0.00000000	0.00000000	9.83483600

16 (C_2, ^{1}A)

K	0.00000000	-0.00000000	-1.50680608
K	0.00679936	-3.55345095	-0.59008950
K	-0.00679936	3.55345095	-0.59008950
K	0.00000000	-0.00000000	2.61910792

H	0.00000000	-0.00000000	5.10214892
H	0.84308970	-1.64499862	0.66658614
H	-0.84308970	1.64499862	0.66658614
H	-0.77341525	-2.38674406	-2.57282764
H	0.77341525	2.38674406	-2.57282764

17 (D_2, ^{1}A)

K	0.00000000	0.00000000	2.49884000
K	0.00000000	0.00000000	6.12764100
K	0.00000000	0.00000000	-2.49884000
K	0.00000000	0.00000000	-6.12764100
H	0.10000000	1.84847900	4.54779300
H	-0.10000000	-1.84847900	4.54779300
H	0.00000000	0.00000000	0.00000000
H	1.84847900	0.10000000	-4.54779300
H	-1.84847900	-0.10000000	-4.54779300

18 (C_{2v}, ^{1}A$_1$)

K	0.00000000	0.00000000	-3.83537314
K	-1.60409600	0.00000000	-0.25089024
K	1.60409600	0.00000000	-0.25089024
K	0.00000000	0.00000000	4.37691507
H	0.00000000	0.00000000	6.77784113
H	0.00000000	0.00000000	1.82811674
H	0.00000000	-1.59048997	-1.54250590
H	-0.00000000	1.59048997	-1.54250590
H	0.00000000	0.00000000	-6.27641349

19 (C_{2v}, ^{1}A$_1$)

K	0.00000000	4.55984875	-1.50875831
K	0.00000000	-4.55984875	-1.50875831
K	1.74705302	-0.00000000	1.54366804
K	-1.74705302	-0.00000000	1.54366804
H	0.00000000	6.47702108	-2.83132333
H	0.00000000	2.12387112	0.16548189
H	0.00000000	0.00000000	4.00511312
H	0.00000000	-2.12387112	0.16548189
H	0.00000000	-6.47702108	-2.83132333

20 (C_{2v}, ^{1}A$_1$)

K	0.00000000	-4.37679391	-0.12409055
K	0.00000000	-0.00000000	-1.77514875
K	0.00000000	-0.00000000	1.97062225
K	-0.00000000	4.37679391	-0.12409055

H	0.00000000	-6.29763135	-1.54127534
H	0.00000000	-1.82554239	-0.14755355
H	0.00000000	-0.00000000	4.37910225
H	-0.00000000	1.82554239	-0.14755355
H	-0.00000000	6.29763135	-1.54127534